Low-Frequency Response of a Multi-Stage Dry-Electrode ECG Bioelectric Amplifier

M. J. BURKE
Dept. of Electronic and Electrical Engineering,
Trinity College, University of Dublin,
College Green, Dublin 2,
IRELAND.
mburke@tcd.ie htpp://www.tcd.ie/eleceng/

K. KOFLER
Dept. of Engineering and IT, Medical Engineering,
Carinthia University of Applied Sciences,
9020 Klagenfurt,
AUSTRIA.
Kerstin.Kofler@edu.fh-kaernten.ac.at https://www.fh-kaernten.at/en

Abstract: - This paper reports the optimisation of the low-frequency response of a multi-stage bioelectric amplifier intended for use in the measurement of the electrocardiogram (ECG) using un-gelled electrodes. The frequency response was optimised to meet the International Electrotechnical Commission 60601 performance standards for electrocardiographs [1,2]. The low frequency response of a multi-stage amplifier configuration was optimised to meet both time and frequency domain specifications. The optimum circuit configuration was found to be two differential stages with a gain of 20dB each and a differential-to single-ended output stage with unity gain. The -3dB pole is placed at 0.028Hz and a zero at 0.0028Hz in the first and second stages giving an overall -3dB bandwidth of 0.043Hz. The pole of the input ac coupling network was placed at 0.0028Hz in order to meet the undershoot and recovery slope requirements in the response to a narrow pulse.

Key-Words: - Electrode Impedance, Un-gelled electrodes, Heart rate monitoring, ECG amplifier.

1 Introduction

The low-frequency response of the bioelectric amplifier used in recording the human electrocardiogram (ECG) is of the utmost importance due to the clinical significance of such recordings. Appropriate magnitude and phase responses are needed in order to prevent distortion of the ECG signal profile and adverse changes in the waveform morphology. The nature of the distortion which can arise in the ECG signal due to poor low frequency response in the recording amplifier has been well documented for several decades and has serious diagnostic implications [3, 4]. The type of distortion which results from poor low frequency response has a detrimental effect primarily on the T-wave, the S-T segment and the Q-T interval.

In addition to hospital oriented ECG recorders, there has been a substantial increase in recent years in the number of portable ECG recorders. Many of these are used in non-clinical scenarios such as general practice, sports medicine, physiology and even on the factory floor. This has led to an increase in battery-operated and low-power equipment with the associated changes in instrumentation design. Consequently trends have changed in the design of the electronic amplifiers for ECG recording. Lower power supply voltages have tended to make amplifier front-end stages ac coupled rather than dc coupled as in the past. This allows electrode polarisation voltages to be eliminated at the input so that they do not saturate the front-end stage of the amplifier. Recent advances in electrode technology have increased the magnitude of these polarisation voltages. Ac coupling also facilitates maintaining a high gain in the early stages of the amplifier to preserve the signal-to-noise ratio. Low-power technology has meant that the gain-bandwidth product of operational amplifiers has fallen so that the gain required in ECG amplifiers is often spread over several stages. This has led to an increase in multi-stage amplifier configurations and a consequent increase in the complexity of the associated frequency response at both the high and low ends of the spectrum. The authors have

concentrated the effort in this paper on investigating the optimisation of the low-frequency response of a multi-stage bioelectric amplifier intended for use in ECG signal recording with gel-free electrodes.

2 Background

Standards for the performance requirements of ECG recorders have been developed in the US by the American National Standards Institute (ANSI) with recommendations made by the American Heart Association (AHA) and in Europe by the International Electrotechnical Commission (IEC). These have changed much over the decades since they were first introduced and have taken account of technological developments. Most recent standards have made an effort to merge the US and EU requirements to make them almost identical. This has, in fact, added strength to both sets of standards and increased the usage of the IEC 60601 standard, which is now accepted worldwide [1,2].

2.1 Frequency domain requirements

Early standards for ECG recorder performance were based on recommendations issued by the AHA and the IEEE in 1967 [5,6]. These standards required that the magnitude of the frequency response be within ± 0.5 dB of the mid-band gain within the frequency range 0.67Hz–150Hz. The low-frequency value was based on a practical lowest heart rate value of 40 beats-per-minute (bpm). The phase shift was required to be no greater than that caused by a single-pole high-pass filter having a -3dB cut-off frequency of 0.05Hz [5,6]. These magnitude and phase response requirements are shown in Fig.1.

More recent standards issued by both the EU and the US [1,2] require that the amplitude response of an ambulatory ECG recorder shall be within ±3 dB of the response at 5Hz, within a frequency band of 0.05Hz to at least 55Hz. A phase response requirement is not specified but the merits of a single-pole high-pass filter having a cut-off frequency of 0.05Hz are still cited as example. Instead of the phase response requirement a time-domain specification has been introduced.

2.2 Time domain requirements

The IEC 60601 most recent standards, which are now closely aligned and merged with those of ANSI, have introduced two time-domain methods of testing ECG recorder performance. These are both shown in Fig.2. Method A was introduced in a previous IEC standard and allows a maximum baseline undershoot of 0.1mV in the transient

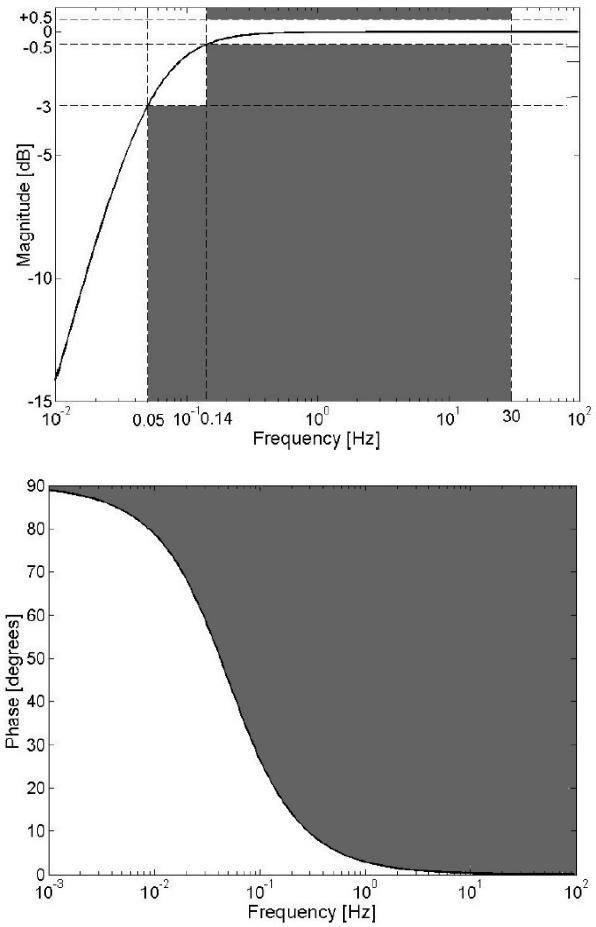

Fig.1 Magnitude and phase requirements.

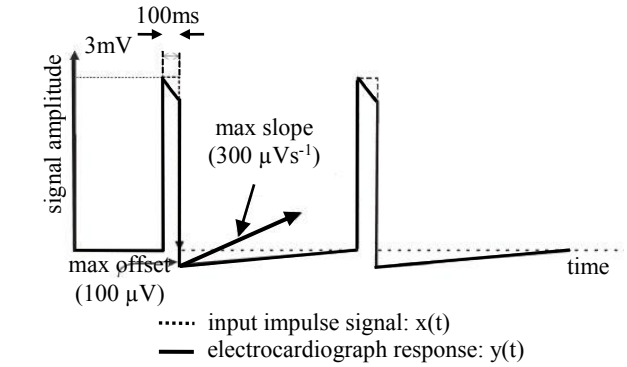

Method A: Rectangular Pulse

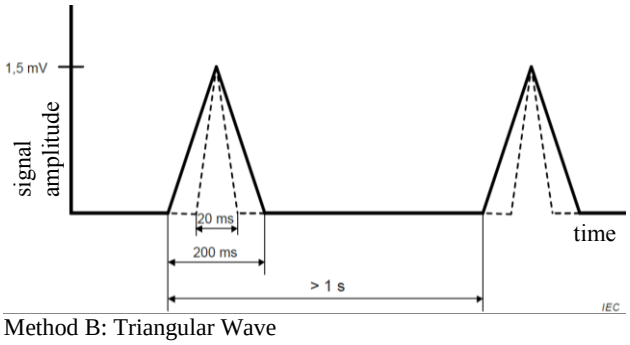

Method B: Triangular Wave

Fig.2 Transient response requirements [1, 2]

response to a narrow rectangular pulse of 3mV amplitude and 100ms duration with a maximum recovery slope of 0.3mV/s between pulses, as can be seen in Fig.2. Method B, on the other hand, uses a triangular wave to model the QRS complex of the ECG. An isosceles triangular wave of peak amplitude of 1.5mV and a duration varying between 20ms and 200ms with a repetition rate of less than 1Hz is applied as input to the recorder. The amplitude of the peak of the triangle must maintain a variation within +0dB and -1dB (-10%) as the pulse duration is varied between 20ms and 200ms. This can be seen in Fig.2. In the studies carried out by the authors, the rectangular pulse of Method A was preferred.

3 Single-stage amplifiers

3.1 Non-inverting unity gain buffer

The simplest single-stage amplifier is the dc coupled non-inverting unity-gain buffer. This is implemented by providing full negative feedback around an op-amp as shown in Fig.3. This stage has a transfer function given as:

$$\frac{V_o}{V_i} = \frac{A(\omega)}{1 + A(\omega)\beta} \tag{1}$$

where A(ω) is the frequency response of the op-amp itself and β is the feedback factor so that β = 1.

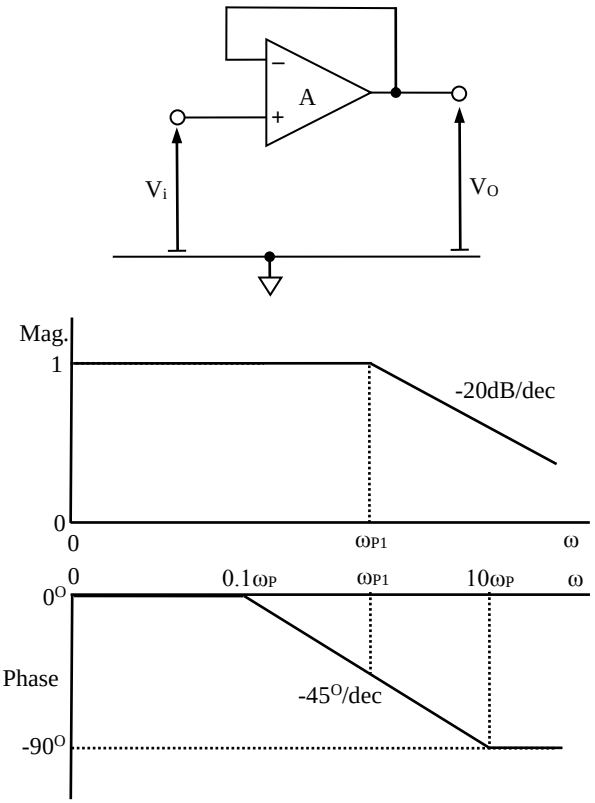

Fig.3. Magnitude & phase of unity gain buffer.

If the op-amp is taken as having a high open-loop gain A_0 at dc and a single pole ω_0 limiting its bandwidth then the transfer function of the buffer amplifier becomes:

$$\frac{V_o}{V_i} = \frac{\dfrac{A_0}{1 + j\left(\dfrac{\omega}{\omega_0}\right)}}{1 + \dfrac{A_0}{1 + j\left(\dfrac{\omega}{\omega_0}\right)}} \tag{2}$$

With $A_0 >> 1$ this simplifies to:

$$\frac{V_o}{V_i} = \frac{1}{1 + j\left(\dfrac{\omega}{A_0\omega_0}\right)} = \frac{1}{1 + j\left(\dfrac{\omega}{\omega_{p1}}\right)} \tag{3}$$

where $\omega_{p1} = A_0\omega_0$ is, in fact, the Gain-Bandwidth product of the op-amp and also represents the -3dB cut-off frequency of the unity gain buffer where the gain has fallen to a value of √2. Bode plots of the magnitude and phase of this transfer function are shown in Fig.3 where it can be seen that the finite gain-bandwidth product of the op-amp limits the radian frequency at which the amplifier operates effectively as a unity gain buffer to ω_{p1}. It also introduces a phase shift which begins to deviate from zero at a frequency a decade below the -3dB point at $0.1\omega_{p1}$ and reaches its final asymtotic value of -90^O at a frequency a decade above the -3dB point at $10\omega_{p1}$. The phase has a value of -45^O at ω_{p1}.

3.2 DC coupled Non-inverting amplifier

The unity gain buffer of Fig.3 can be converted into a simple dc-coupled non-inverting gain stage as shown in Fig.4, by including the feedback network composed of resistors R_1 and R_2 in order to reduce the feedback factor β to less than unity. This stage has a transfer function given by:

$$\frac{V_o}{V_i} = \frac{R_1 + R_2}{R_1} \frac{1}{1 + j\left(\dfrac{\omega(R_1 + R_2)}{A_0\omega_0 R_1}\right)} = \frac{A_{V0}}{1 + j\left(\dfrac{\omega}{\omega_c}\right)} \tag{4}$$

where $A_{V0} = (R_1+R_2)/R_2$ is the dc closed-loop gain determined by the feedback network and the pole is located at $\omega_c = A_0\omega_0/A_{V0}$. Plots of the magnitude and phase of the transfer function are also shown in Fig.4. From this it can be seen that the -3dB bandwidth of the non-inverting gain stage is determined by the gain bandwidth product of the op-

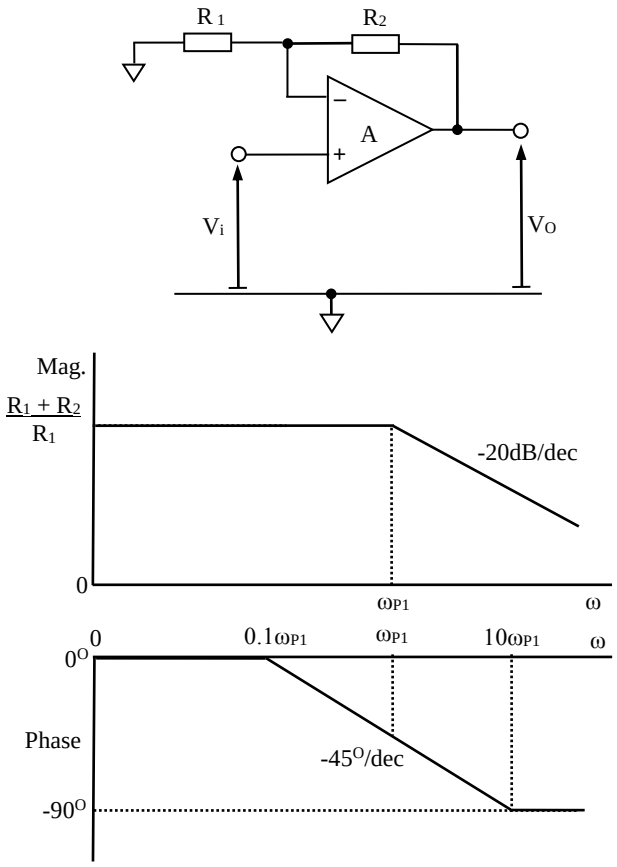

Fig.4. Magnitude and phase of dc gain stage.

amp scaled down by a factor of the closed loop gain. In very low-power op-amps, the gain-bandwidth product is often extremely limited which means that even if a moderately high gain amplifier is required it often must be constructed of several stages. This is particularly true in the case of bioelectric amplifiers and also has implication for the low-frequency response of these amplifiers.

3.3 AC coupled unity gain high-pass filter

In biomedical applications the dynamic signal of interest is often superimposed on a large dc or very low-frequency baseline and consequently ac coupling is required to suppress the latter. AC coupling can be added to the unity gain buffer by simply including the network consisting of resistor R_3 and capacitor C_3 at the input as shown in Fig.5. This effectively creates a simple 1st-order unity-gain high-pass filter. This configuration was used as the reference standard in the early performance specifications [5,6] where the -3dB cut-off frequency was set at 0.05Hz. It is still cited as a comparative reference in more recent specifications [1,2]. If the gain bandwidth of the op-amp is considered as unlimited for convenience in this case

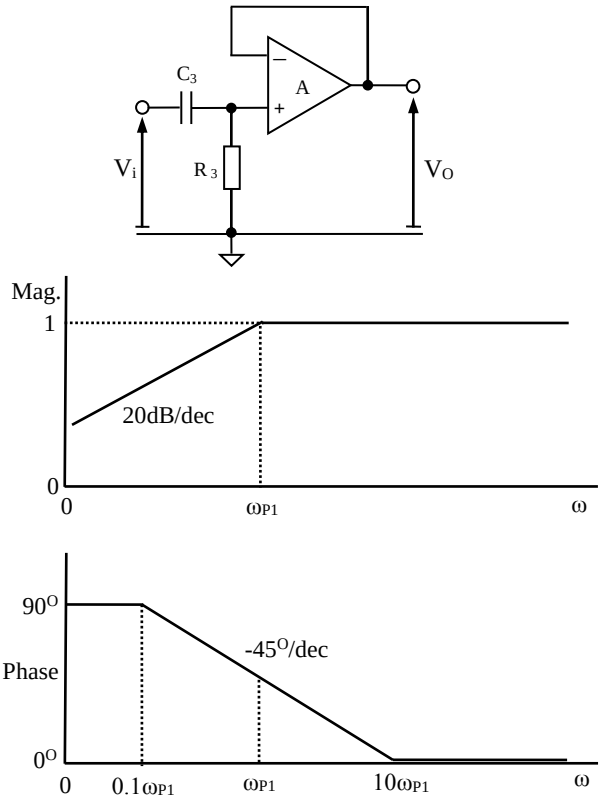

Fig.5. Magnitude & phase response of 0.05Hz HPF.

then the steady-state transfer function of this stage is given as:

$$\frac{V_o}{V_i} = \frac{j\omega C_3 R_3}{1 + j\omega C_3 R_3} = \frac{j\left(\dfrac{\omega}{\omega_{P1}}\right)}{1 + j\left(\dfrac{\omega}{\omega_{P1}}\right)} \qquad (5)$$

where the radian pole frequency is $\omega_{p1} = 1/C_3R_3$. There is also a theoretical zero located at $\omega = 0$. Idealised Bode plots of the magnitude and phase of the frequency response are also shown in Figure 5. The high-frequency pass-band gain is unity.

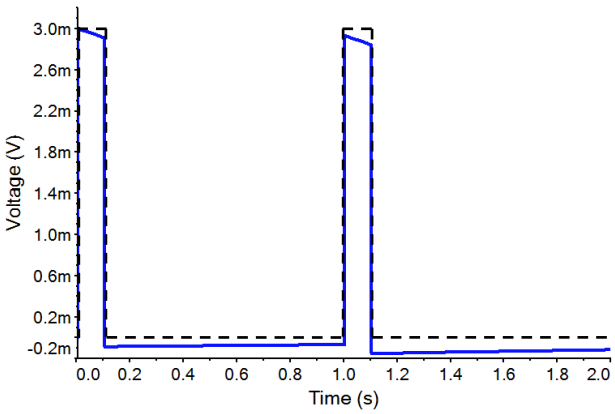

Fig.6. Narrow pulse response of 0.05Hz HPF

The pole at radian frequency $\omega_{P1} = 1/C_3R_3$ corresponds to the -3dB cut-off frequency of the high-pass response. The response of this filter in the time domain to the narrow input pulse which is defined in Fig.2 can be seen in Fig.4. The undershoot in the response is 0.093mV and the recovery slope is 29μV/s. This indicates that this filter meets the required international performance criteria for ECG amplifiers in the time domain.

3.4 Inverting AC Coupled HPF Gain Stage

The next stage of interest is the 1st-order amplifier stage having a high-pass response as shown in Fig.7. This stage is ac coupled but has a gain in the pass band and is also an inverting stage. This stage has a

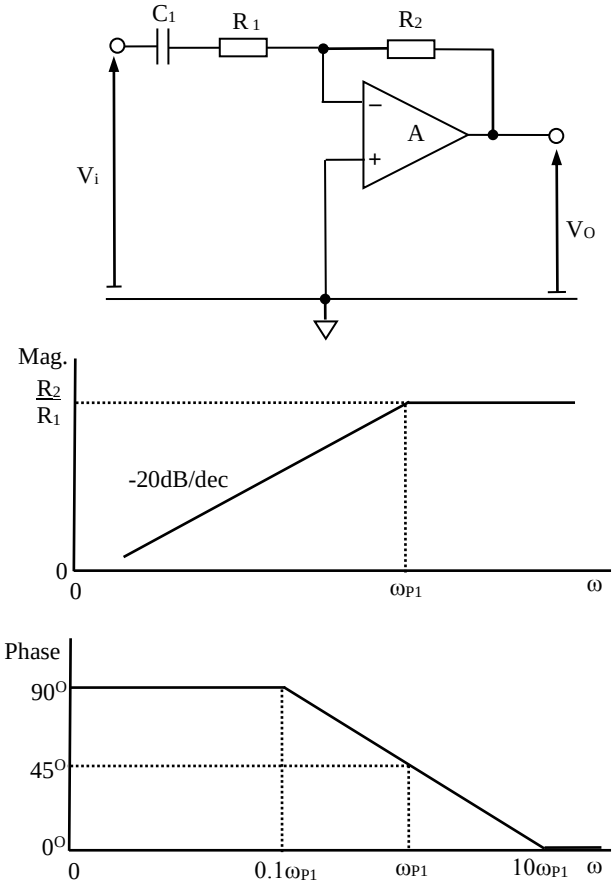

Fig.7. Magnitude & phase of inverting amplifier

steady-state transfer function given by:

$$\frac{V_o}{V_i} = -\frac{j\omega C_1 R_2}{(1+ j\omega C_1 R_1)} = -\frac{R_2}{R_1}\frac{j\omega C_1 R_1}{(1+ j\omega C_1 R_1)} \qquad (6)$$

This stage can be seen to have a frequency response almost identical to the ac coupled unity-gain buffer as shown by the magnitude and phase Bode plots given in Fig.7. The transfer function of this stage is of the form:

$$\frac{V_o}{V_i} = A_{V0}\frac{j\left(\frac{\omega}{\omega_{P1}}\right)}{\left[1+ j\left(\frac{\omega}{\omega_{P1}}\right)\right]} \qquad (7)$$

where $A_{V0} = -R_2/R_1$ and $\omega_{p1} = 1/C_1R_1$.

This response characterises a single-pole high-pass filter which provides in-band amplification but with inversion. Note that the 180O phase shift associated with this inversion is omitted from the phase plot of Fig.7.

3.5 Non-Inverting High-Pass Gain Stage

The inverting amplifier stage can be modified to be a non-inverting stage if the input signal is applied to the non-inverting input of the op-amp instead of to capacitor C_1 as shown in the circuit of Fig.8.

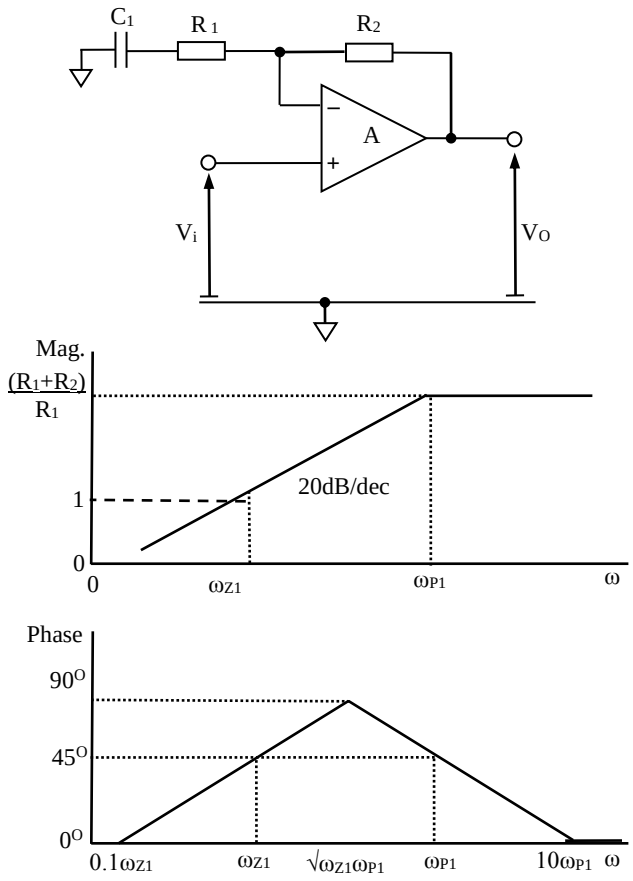

Fig.8. Magnitude & phase of non-inverting amp

The transfer function of this stage is given as:

$$\frac{V_o}{V_i} = \frac{[1 + j\omega C_1(R_1 + R_2)]}{(1+ j\omega C_1 R_1)} = \frac{1+ j\left(\frac{\omega}{\omega_{Z1}}\right)}{1+ j\left(\frac{\omega}{\omega_{P1}}\right)} \qquad (8)$$

where $\omega_{p1} = 1/C_1R_1$ and $\omega_{z1} = 1/C_1(R_1+R_2)$

Bode plots of the magnitude and phase of the transfer function are included in Fig.8. It can be seen that the in-band high-frequency gain is given for $\omega \to \infty$ as $A_{V0} = (R_1 + R_2)/R_1$. The pole location ω_{p1} defines the -3dB cut-off frequency for the high-pass filter response. However, it should be noted that at the location of the zero, ω_{z1}, the magnitude of the gain becomes unity and remains at this down to dc. This means that there is no rejection of low-frequency artefact or baseline drift. Conversely it does allow a dc bias voltage level to be maintained and passed on to a subsequent amplifier stage. It should also be noted that the ratio of the locations of the pole and zero frequencies is equal to the closed-loop mid-band gain of the amplifier, i.e. $\omega_{p1}/\omega_{z1} = A_{V0}$.

The phase can be seen to be zero at low frequencies, then to rise at a rate of 45^O/dec from a frequency of $0.1\omega_{z1}$ a decade below the location of the zero. It reaches its maximum value at a frequency of $\sqrt{\omega_{z1}\omega_{p1}}$ which is the geometric mean of the pole and zero locations. The phase then decreases thereafter at a rate of -45^O/dec returning to zero at a frequency of $10\omega_{p1}$ a decade above the location of the pole. If the pole and zero locations are separated by more than two decades the phase will reach a plateau at 90^O between the frequencies a decade above the location of the zero, $10\omega_{z1}$ and a decade below the location of the pole, $0.1\omega_{p1}$.

3.6 AC coupled high-pass gain stage

The final single-stage amplifier of interest is an amplifying stage with a 1st-order high-pass frequency response which includes ac coupling on the input in the form of the resistor R_3 and the capacitor C_3 to block dc voltages and suppress low-frequency artefact and baseline drift. The schematic diagram of this stage is shown in Fig.9. This stage has a steady-state transfer function of the form:

$$\frac{V_o}{V_i} = \frac{j\omega C_3 R_3 [1 + j\omega C_1 (R_1 + R_2)]}{(1 + j\omega C_3 R_3)(1 + j\omega C_1 R_1)} \qquad (9)$$

It can be seen that this stage has an in-band high-frequency gain of $A_V = (R_1 + R_2)/R_1$. The -3dB pole in the high-pass response is again located at a radian frequency of $\omega_{P1} = 1/C_1R_1$. As for the previous circuit, there is a zero in the response located at a frequency of $\omega_{Z1} = 1/C_1(R_1 + R_2)$. There is also, however a second pole introduced by the input coupling network and located at a frequency given by $\omega_{P2} = 1/C_3R_3$. The transfer function of this stage can therefore also be can be written as:

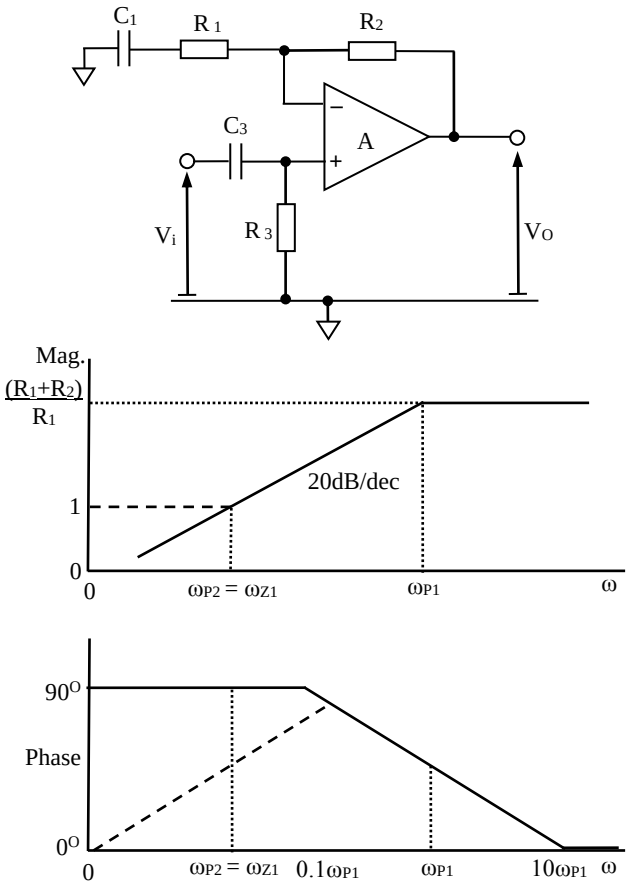

Fig.9. Magnitude & phase of 1-stage amplifier

$$\frac{V_o}{V_i} = \frac{j\left(\frac{\omega}{\omega_{Z1}}\right)\left[1 + j\left(\frac{\omega}{\omega_{Z1}}\right)\right]}{\left[1 + j\left(\frac{\omega}{\omega_{P1}}\right)\right]\left[1 + j\left(\frac{\omega}{\omega_{P2}}\right)\right]} \qquad (10)$$

Bode plots of the magnitude and phase of this stage are also shown in Fig.9. If the input ac coupling network C_3-R_3 were omitted, the gain of this stage would level out at unity, at the zero in the frequency response which is located at a radian frequency of $\omega_{Z1} = 1/C_1(R_1 + R_2) = \omega_{P1}/A_{V0}$ as shown by the dashed line in the magnitude response of Fig.9. The zero would also have the effect of restoring the low-frequency phase back to zero as $\omega \to 0$, as again shown by the dashed line in the phase response of Fig.9.

The effect of the second pole introduced by the coupling network is to ensure that the magnitude attenuation continues down through low frequencies to dc which blocks these components. It also means that the low-frequency phase shift levels out at 90^O and does not return to zero. This can be seen from the solid line plots of Fig.9. In order to get an overall response in the form of an ideal high-pass

filter, the lower frequency pole, ω_{P2}, of the input network is arranged to cancel the zero in the response of the feedback network by a choice of time constants such that $C_3R_3 = C_1(R_1 + R_2)$. In this case the transfer function of the stage becomes:

$$\frac{V_o}{V_i} = \frac{j\omega C_3 R_3}{(1 + j\omega C_1 R_1)} = \frac{j\omega C_1 (R_1 + R_2)}{(1 + j\omega C_1 R_1)} \qquad (11)$$

This is depicted by the solid line responses in Fig.9.

It was decided to explore whether or not the frequency response of the single high-pass stage could be improved by not implementing an exact cancelation of the pole and zero, but to allow a degree of mismatch in their locations. In particular the effect on the phase of varying the location of the second pole on either side of the zero was of interest. Fig.10 shows plots of the magnitude and phase responses of a single-stage high-pass amplifier having a non-inverting gain of 20dB.

An ideal op-amp model was used in MultiSim for circuit simulations so that its properties would not influence the results. The heavy curves in Figure 10 represent the case where $C_3R_3 = C_1(R_1 + R_2)$ with precise pole-zero cancellation. Moving the location of the second pole above that of the zero increases the phase above the phase of the perfect cancellation curve, and also raises the -3dB cut-off frequency, which does not improve the response. Moving the location of the second pole below that of the zero, on the other hand, lowers the phase compared with the perfect cancellation curve by a small amount at in-band frequencies and lowers the frequency at which the gain falls from 0dB. However, even when the frequency of the second pole is lowered significantly, there is only a small reduction of the phase at in-band frequencies. The very small benefits gained in phase may be outweighed by the increased initialisation time of the amplifier due to the time-constants involved. Fig.10 also shows the effect of varying the second pole location on the response to the narrow pulse of 3mV amplitude and 100ms duration. It can be seen that lowering the frequency of the pole location gives a slight reduction in undershoot and recovery slope of the pulse response, which are again only marginal and not a highly significant improvement.

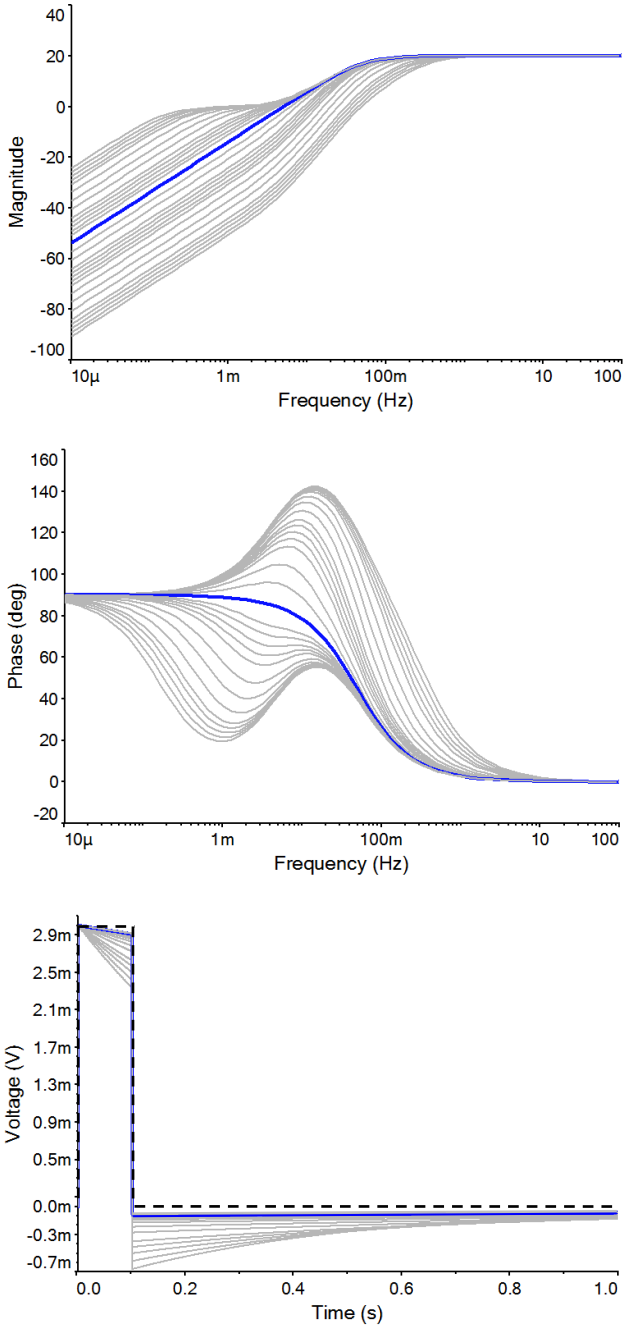

Fig.10 Response of 1-stage amp to 2nd pole placing

4 Multi-stage amplifiers

4.1 Two-stage differential amplifier

The schematic diagram of a simple differential amplifier is shown in Fig.11. This has a single cross-coupled input stage with differential input voltages V_1 and V_2. This is followed by the standard differential-to-single-ended conversion stage which provides the output voltage, V_O. The A and B designation of components will nominally have the same values. The steady-state transfer function of this amplifier structure is given for a differential input $V_1 - V_2$ as:

$$\frac{V_o}{V_1 - V_2} = \frac{R_5}{R_4} \frac{[1 + j\omega C_1 (R_1 + 2R_2)] j\omega C_3 R_3}{(1 + j\omega C_1 R_1)(1 + j\omega C_3 R_3)} \qquad (12)$$

Very often $R_5 = R_4$ so that the output stage has unity gain, to maximize the CMRR.

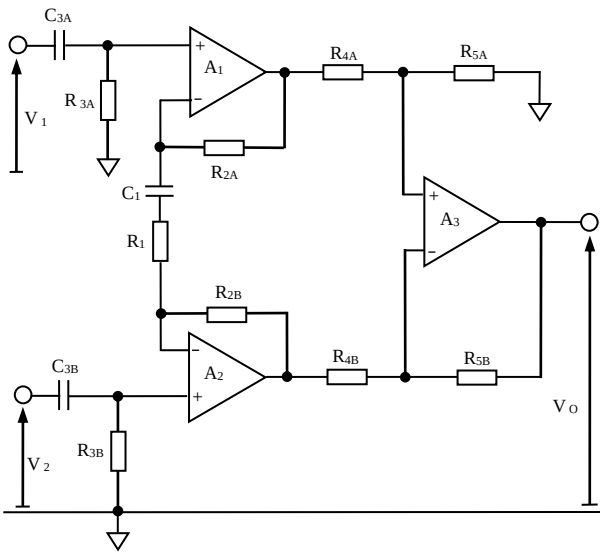

Fig.11 Schematic diagram of differential amplifier

In this case the in-band differential gain of this stage is given as $A_{V0} = (R_1 + 2R_2)/R_1$. The -3dB cut-off frequency is again located at $\omega_{P1} = 1/C_1R_1$ while the zero is located at $\omega_{Z1} = 1/C_1(R_1 + 2R_2) = \omega_{P1}/A_{V0}$. The pole due to the input ac coupling network, which is identical at each input terminal, is again located at a frequency $\omega_{P2} = 1/(C_3R_3)$. The same pole-zero cancellation as implemented in the single stage amplifier can be obtained in the differential amplifier by choosing $C_3R_3 = C_1(R_1 + 2R_2)$. Plots of the magnitude and phase of the two stage differential amplifier are shown in Fig.12. Varying the location of the pole ω_{p2} has the same effect as in the equivalent single stage amplifier. The curves therefore show only two unmatched locations for the second pole, one at the geometric mean of the main pole ω_{P1} and the zero ω_{Z1} that is at a frequency $\omega = \sqrt{\omega_{P1}\omega_{Z1}}$ and the other below the zero by the same factor as the geometric mean is above it. The pulse response of Fig.13 shows the detail at the lower end of the trailing edge of the pulse. It can be seen that there is little benefit to be gained from lowering the location of the second pole and it has negligible effect on the undershoot and recovery slopes. Increasing the frequency of the pole location causes the undershoot to exceed 100μV and the recovery slope to exceed 300μVs^{-1}, thereby violating the performance requirements. It therefore makes most sense to apply the exact pole-zero cancellation principle as in the case of the single-stage amplifier and choose $C_3R_3 = C_1(R_1 + 2R_2)$.

4.2 Three-stage differential amplifier

The final configuration of interest is the 3-stage differential amplifier shown in Fig.14. This has a high-pass input stage with a differential-to-single-

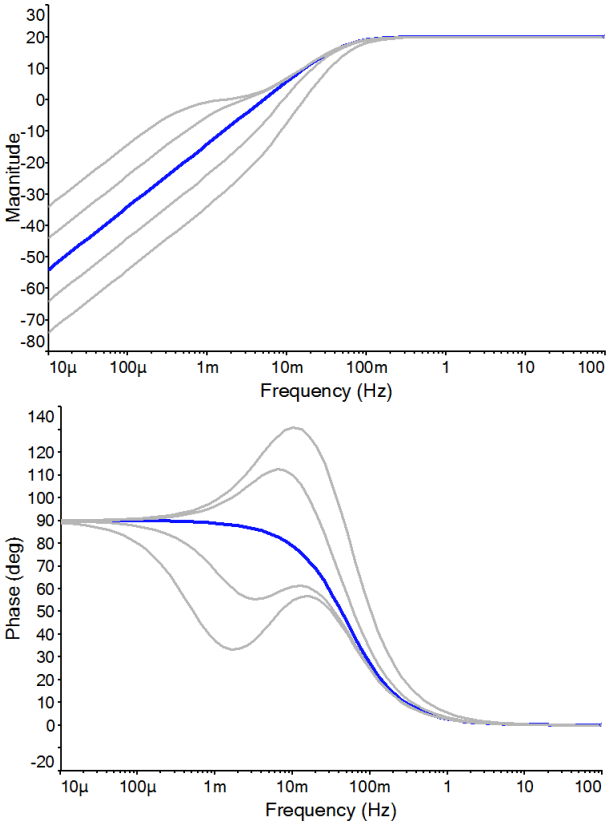

Fig.12 Magnitude & phase of 2-stage amplifier

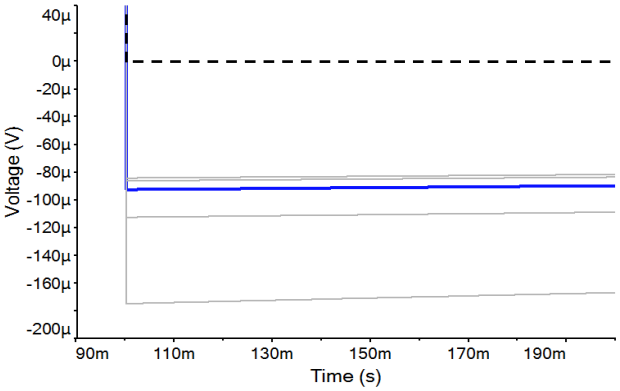

Fig.13 Trailing edge response of 2-stage amplifier

ended output stage identical to the two stage amplifier. There is a second differential stage which is dc coupled to the first so that the output dc bias potentials of the first stage will carry through to the second stage. The ac coupling of the first stage is sufficient to block any dc polarisation potentials at the input. The steady state transfer function of this three stage amplifier is given as:

$$\frac{V_o}{V_1 - V_2} = \frac{R_5}{R_4} \times \frac{[1 + j\omega C_1(R_1 + 2R_2)][1 + j\omega C_7(R_7 + 2R_6)]j\omega C_3R_3}{(1 + j\omega C_1R_1)(1 + j\omega C_7R_7)(1 + j\omega C_3R_3)} \quad (13)$$

where, R_6, R_7 and C_7 are the components in the second differential stage. It can be seen that the dc coupling in the second differential stage adds an additional pole and zero to the transfer function. If the output stage has unity gain and the overall gain is shared equally between the two differential stages then the poles and zeros of both of these stages are identical so that $\omega_{P1} = 1/(C_1R_1) = \omega_{P3} = 1/(C_7R_7)$ and $\omega_{Z1} = 1/[C_1(R_1 + 2R_2)] = \omega_{P1}/A_{V1} = \omega_{Z2} = 1/[C_7(R_7 + 2R_6)] = \omega_{P3}/A_{V2}$. The gains of the individual differential stages were maintained at 20dB, as for the two-stage amplifier, so that the overall gain of the three-stage amplifier is 40dB. On the basis of the results of Fig.10 and Fig.11 for the two-stage amplifier the pole-zero cancellation was maintained in the first differential stage by the choice $C_3R_3 = C_1(R_1 + 2R_2)$. If the intention, in the first instance, is to maintain the -3dB frequency of the three-stage amplifier at the same location as for the two-stage amplifier then it can be shown that:

$$\omega_{-3dB2} = \sqrt{\sqrt{2} - 1}\ \omega_{-3dB1} = 0.645\,\omega_{-3dB1} \qquad (14)$$

where ω_{-3dB2} is the -3dB frequency of a single differential stage in a two-stage cascade having identical stages and ω_{-3dB1} is the -3dB frequency of a single-stage differential amplifier in isolation. The overall -3dB frequency of the two cascaded differential stages should be equal to the -3dB high-pass cut-off frequency required in the amplifier as a whole. From eq.14, it can be established that with f_{-3dB1} = 0.05Hz then f_{-3dB2} = 0.032Hz to maintain an overall -3dB frequency of 0.05Hz in the three-stage amplifier. However, while this choice will satisfy the frequency-domain performance requirements it does not meet the narrow pulse response requirements as indicated in Fig.2. In order to accomplish the latter, it is necessary to lower the overall -3dB frequency of the three-stage amplifier to 0.043Hz which corresponds to a -3dB frequency for the individual differential stages of 0.028Hz. When this is done, the undershoot in the pulse response is maintained at 98μV and the recovery slope at 15μVs^{-1}. Fig.10 shows the magnitude and phase responses of the 3-stage ECG as illustrated by the upper blue curves. The lower heavy grey curves represent the corresponding responses of a single-stage amplifier with a -3dB frequency of 0.05Hz shown for comparison. The time-domain response to the narrow 3mV-100ms pulse expanded in the region of the undershoot is shown in Fig 11. Again the heavy blue curve indicates the response of the 3-stage ECG amplifier while the heavy grey curve indicates the response of a single-stage amplifier with a -3dB cut-off frequency of 0.05Hz for comparison. These responses fall within the limits specified by international performance standards for ECG recording equipment.

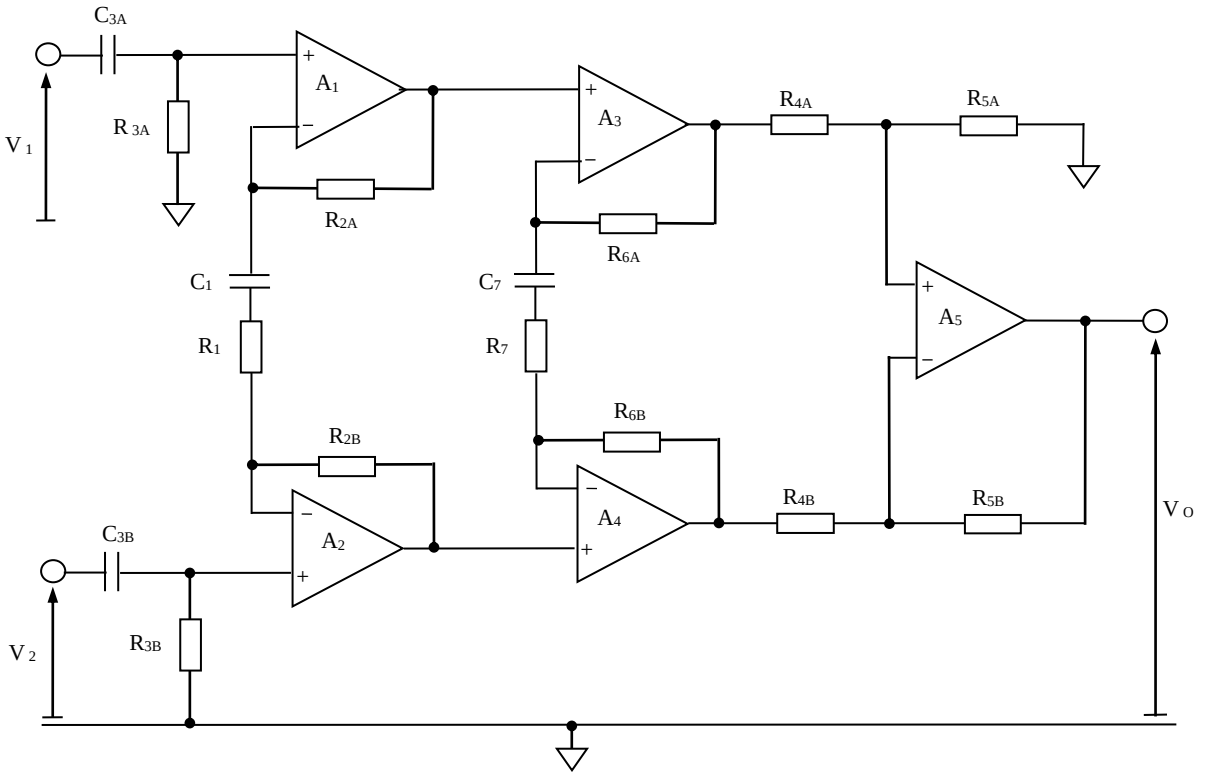

Fig.14 Schematic diagram of a 3-stage ECG amplifier.

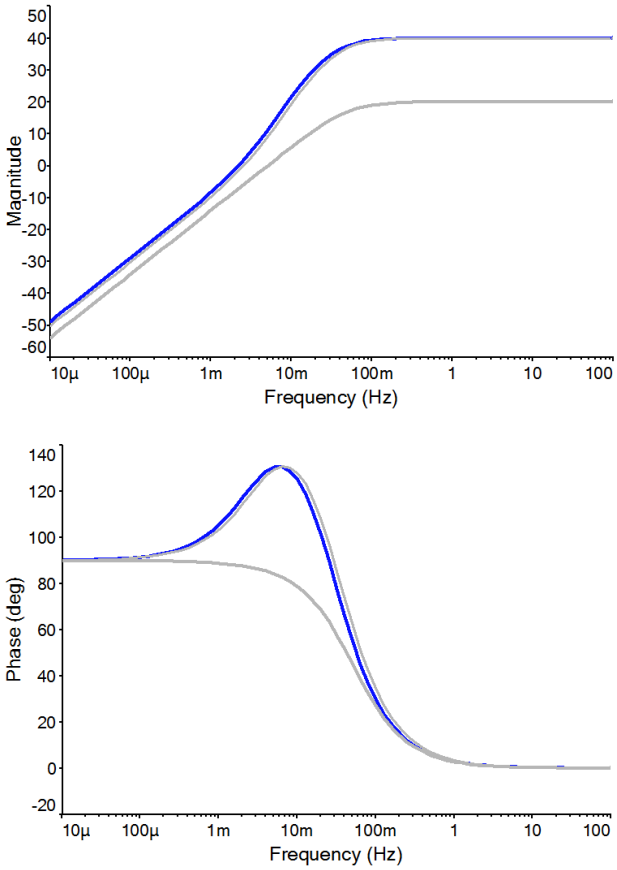

Fig.15 Magnitude & phase of 3-stage ECG amp

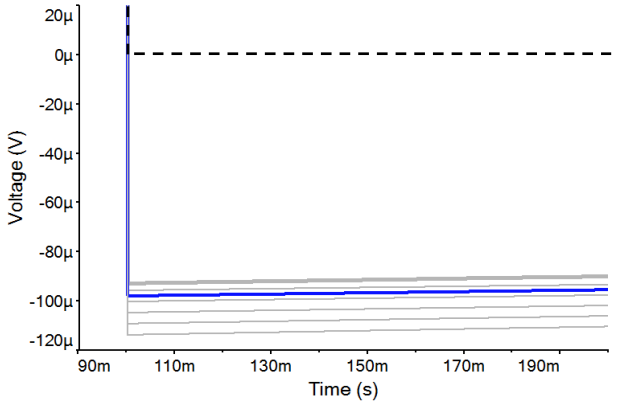

Fig.16 Pulse response of 3-stage ECG amplifier

5 Conclusion

A 3-stage ECG amplifier for use with un-jelled electrodes has been designed which satisfies the IEC 60601 specification. The undershoot in the pulse response is less than 100µV and the recovery slope less than $300\mu Vs^{-1}$. The -3dB low cut-off frequency of two identical cascaded differential stages must be set at 0.028Hz in order to accomplish this. The magnitude, phase and narrow pulse responses of this amplifier have been contrasted against those of a single-stage amplifier having a -3dB cut-off frequency of 0.05Hz. These principles can be applied in the design of very low power ECG amplifiers intended for use with dry un-gelled electrodes such as those previously reported [7-10].

References:

[1] International Electrotechnical Commission, *Medical Electrical Equipment Std.* 2-25. IEC 60601, 2011.

[2] International Electrotechnical Commission, *Medical Electrical Equipment Std.* 2-47. IEC 60601, 2012.

[3] A. S. Berson and H. V. Pipberger, The Low-Frequency Response of Electrocardiographs, A Frequent Source of Recording Errors, *Amer. Heart J.*, 71, 779-789, 1966.

[4] D. Tayler and R. Vincent, Signal distortion in the electrocardiogram due to inadequate phase response, *IEEE Trans. Biomed. Eng.*, 30, 352-356, 1983.

[5] C. E. Kossmann et al., Recommendations for standardization of leads and of specifications for instruments in electrocardiograpy and vectorcardiography, *Circulation*, 35, 583–602, 1967.

[6] H. V. Pipberger et al., Recommendations for standardization of instruments in electrocardiography and vectorcardiograhy, *IEEE Trans. Biomed. Eng.*, 14, 60-68, 1967.

[7] Assambo, C., Burke, M. J., An Optimized High-Impedance Amplifier for Dry-Electriode ECG Recording, *NAUN Int. J. Circuits, Systems & Signal Processing*, 6, 332-341, 2012.

[8] Burke, M. J., Assambo, C., An Ultra-Low Power Dry-Electrode ECG Amplifier Having Optimized Low-Frequency Response and CMRR, *Proc. 16th WSEAS Int. Conf. on Circuits*, Kos, 2012, paper. no. 68101 – 025.

[9] Burke, M. J., Assambo, C., An Ultra-Low Power Dry-Electrode ECG Amplifier Having Optimized Low-Frequency Response and CMRR, in editor(s) Balas, V. E., Koksal, M., *Recent Researches in Circuits & Systems*, WSEAS, Athens, 2012, pp54-59.

[10] Assambo, C., Burke, M., Low-Frequency Response and the Skin-Electrode Interface in Dry-Electrode Electrocardiography, in editor(s) Millis, R. M., *Advances in Electrocardiograms - Methods and Analysis*, online, InTech, 2012, pp23 – 52.